

ORIGINAL ARTICLE

## Metformin plus sorafenib highly impacts temozolomide-resistant glioblastoma stem-like cells

Mihaela D. Aldea<sup>1\*</sup>, Bobe Petrushev<sup>1\*</sup>, Olga Soritau<sup>2</sup>, Ciprian I. Tomuleasa<sup>1</sup>, Ioana Berindan-Neagoe<sup>1</sup>, Adriana G. Filip<sup>3</sup>, Gabriela Chereches<sup>2</sup>, Mihai Cenariu<sup>4</sup>, Lucian Craciun<sup>1</sup>, Corina Tatomir<sup>2</sup>, Ioan-Stefan Florian<sup>5</sup>, Carmen B. Crivii<sup>6†</sup>, Gabriel Kacso<sup>7†</sup>

<sup>1</sup>Research Center for Functional Genomics, Biomedicine and Translational Medicine, University of Medicine and Pharmacy Iuliu Hatieganu and Department of Functional Genomics, the Oncology Institute Prof. Dr. Ion Chiricuta, Cluj Napoca; <sup>2</sup>Department of Radiobiology and Tumor Biology, Ion Chiricuta Cancer Center, Cluj-Napoca; <sup>3</sup>Department of Physiology, Iuliu Hatieganu University of Medicine and Pharmacy, Cluj-Napoca; <sup>4</sup>Faculty of Veterinary Medicine, University of Agricultural Sciences and Veterinary Medicine, Cluj-Napoca; <sup>5</sup>Department of Neurosurgery, Iuliu Hatieganu University of Medicine and Pharmacy, Cluj-Napoca; <sup>6</sup>Department of Morphological Sciences, Iuliu Hatieganu University of Medicine and Pharmacy, Cluj-Napoca, <sup>7</sup>Department of Oncology and Radiotherapy, Iuliu Hatieganu University of Medicine and Pharmacy, Cluj-Napoca, Romania

\* These authors contributed equally to this work.

† These authors share senior co-authorship.

### Summary

**Purpose:** Glioblastoma stem cells (GSCs), responsible for the dismal disease prognosis after conventional treatments, are driven by overactive signaling pathways, such as PI3K/AKT/mTOR and RAS/RAF/MAPK. The objective of our study was to target *in vitro*-GSCs by combining metformin (Met) as a mTOR inhibitor, with sorafenib (Soraf) as a RAF inhibitor.

**Methods:** GSCs cultured under basal conditions were treated with Met, temozolomide (TMZ), Soraf, Met+TMZ and Met+Soraf; as untreated arm served as control. At 4 hrs of drug exposure, we measured the level of reactive oxygen species (ROS) by 2',7'-dichlorofluorescein diacetate (DCF-DA) assay, apoptosis by proidium iodide (PI)-V Annexin staining and efflux pump activity by using the fluorescent dye rhodamine 123. At 24 hrs, we measured cell proliferation by 3-(4,5-dimethylthiazolyl-2)-2,5-diphenyltetrazolium bromide (MTT) assay, apoptosis and malondialdehyde (MDA) levels. MTT results were compared with corresponding measurements on cultures of non-stem glioblastoma

cells and osteoblasts.

**Results:** Met+Soraf exerted the highest antiproliferative effects in GSCs and non-stem glioblastoma cells ( $p < 0.001$ ). Both Met and Soraf monotherapy exhibited a selective cytotoxic effect on GSCs ( $p < 0.001$ ), while no effect was detected on non-stem glioblastoma cells ( $p > 0.05$ ). Soraf, but not Met, impacted the proliferation of normal cells. Soraf displayed synergism with Met in producing high levels of ROS, decreasing efflux pump activity and generating the highest apoptotic rates when compared to either drug alone ( $p < 0.001$ ).

**Conclusion:** GSCs were highly sensitive to the combination of Met and Soraf which reduced cell proliferation, increased oxidative stress, inhibited efflux pump activity and ultimately killed GSCs. We strongly believe that these results warrant further *in vivo* exploration.

**Key words:** glioblastoma, metformin, sorafenib, stem-like cells, temozolomide

### Introduction

Glioblastoma is a highly infiltrative and deadly tumor of the central nervous system that rapidly spreads within nervous tissues and makes

complete resection illusive in most cases [1,2]. Although the current gold standard treatment consists of a multidisciplinary approach that includes surgery and adjuvant radio-chemotherapy, followed by maintenance chemotherapy with te-

mozolomide [3,4], the median survival rarely exceeds 15 months [5]. The failure of conventional treatments along with the observation that 60-75% of patients derive no benefit from treatment with temozolomide [6], have imposed the urgent need for new treatment strategies.

A major breakthrough in modern neuro-oncology reveals that the aggressive and incurable nature of glioblastoma has been associated with the existence of a small subpopulation of GSCs that have the ability to undergo self-renewal and are resistant to conventional chemo-radiotherapy, thus initiating tumorigenesis and supporting tumor growth [7]. Proposed mechanisms of chemo- and radioresistance in GSCs include the overactivity of various signaling pathways important for the maintenance of the stemness feature, cell growth, proliferation and survival, enhanced DNA repair mechanisms and drug-efflux transporters [8], as well as the preferential localization of GSCs within hypoxic areas [9]. Moreover, the dismal prognosis of glioblastoma is associated with an aberrantly elevated expression or constitutive activation of various tyrosine kinase receptors, such as epidermal growth factor receptor (EGFR) [10,11], vascular endothelial growth factor receptor 2 (VEGFR2) [12], platelet-derived growth factor receptor beta (PDGFRb) [13] or insulin-like growth factor 2 (IGF2) [14]. As a consequence, important roles are provided for the phosphatidylinositol 3-kinase (PI3K)/mammalian target of

rapamycin (mTOR) and mitogen-activated protein kinase (MAPK) pathways in the biology of glioblastoma, as they are downstream pathways activated by the frequently over-expressed receptor tyrosine kinases stated above [15,16].

Taking into account the cooperative function of PI3K/AKT/mTOR and RAS/RAF/MAPK in tumorigenesis and cancer cell proliferation, we propose a novel combination between the mTOR inhibitor, metformin, and the RAF inhibitor, sorafenib, in the treatment of GSCs. Encouraging results have emerged from recent data published on glioblastoma [17-20] and suggest that metformin could be “the most clinically relevant drug ever reported for targeting of glioma-initiating cells” [18], mainly due to mTOR inhibition [21,22]. Sorafenib, a tyrosine kinase inhibitor used in the treatment of hepatocellular and renal cell carcinoma, was also recently proven to inhibit glioblastoma-initiating cells [23] by targeting molecules frequently over-expressed in glioblastoma, such as VEGFR, PDGFR, c-kit or RAF [24], and it may become a promising drug in the treatment of glioblastoma (Figure 1).

In the present study, we show for the first time that metformin and sorafenib could be combined into an efficient *in vitro* treatment strategy that targets GSCs and that this association is superior to either drug used alone or when compared with the gold standard chemotherapy, TMZ.

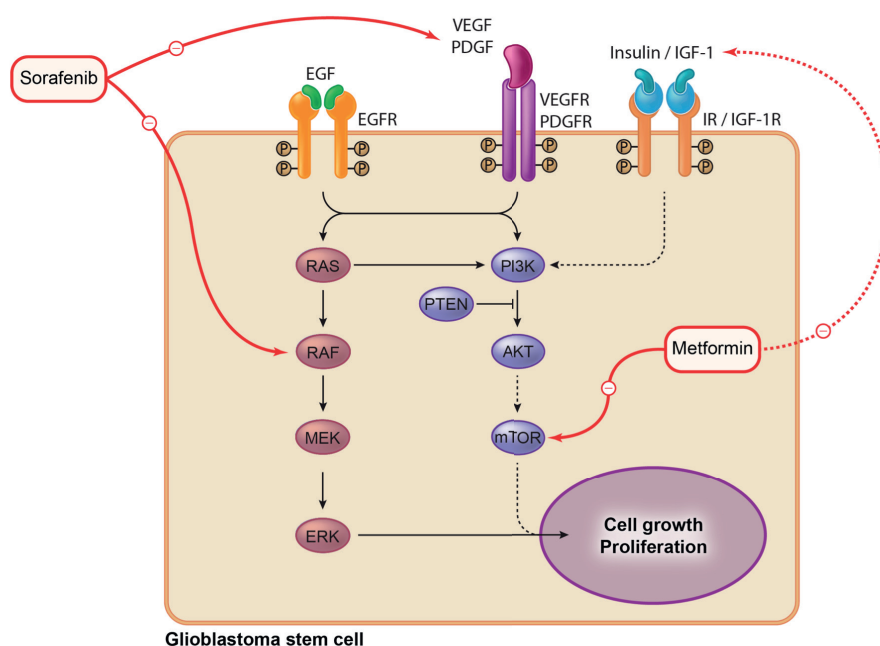


**Figure 1.** Putative molecular targets of sorafenib and metformin in glioblastoma stem cells.

## Methods

### Reagents

Metformin (Wörwag Pharma) was diluted in phosphate buffer solution (PBS) and used in a final concentration of 6 mM, according to the calculated half maximal inhibitory concentration. TMZ (Schering-Plough) was used at a final concentration of 50  $\mu$ M after dilution in Dulbecco's Modified Eagle Medium (DMEM) adjusted at pH of 4.0. Sorafenib (Bayer and Onyx Pharmaceuticals) was prepared as stock solution by dilution in dimethyl sulphoxide and the working solution by dilution in cell medium and used at a final concentration of 2.5  $\mu$ M. Both TMZ and Sorafenib doses corresponded to the clinically relevant concentrations used in patients.

DMEM, high glucose, HAM nutrient F12 medium, streptomycin, penicillin, glutamine, non-essential amino acids, MTT solution, beta-mercaptoethanol, fetal calf serum (FCS) and trypsin were all purchased from Sigma Aldrich (St Louis, MO, USA).

### Cell cultures

GSCs were isolated from a freshly surgically resected human glioblastoma specimen, and cultured in a serum-free medium containing epidermal growth factor (EGF), basic fibroblast growth factor (FGF), and B27 supplement, as previously described [7]. After isolation and expansion, cells were cultured at 37 °C in a humidified atmosphere of 95 % air and 5% CO<sub>2</sub>, in Ham's F-12 and DMEM media used in 1:1 ratio, supplemented with 15% FCS, 100 U/ml penicillin and 100  $\mu$ g/ml streptomycin, 2mM L-glutamine, 1% non-essential amino acids (NEA), 55  $\mu$ M beta-mercaptoethanol and 1 mM sodium pyruvate. Cells were previously shown to express stem cell features, such as CD133, OCT 3/4, CD 90, nestin and nanog, while having also the capacity to form neurospheres in serum-free medium and displaying a high proliferative potential despite chemotherapy and irradiation [7]. Non-stem glioblastoma cells were cultured in the same conditions and in a similar growth medium. Osteoblasts were cultured in complex osteogenic medium consisting of DMEM/F-12 medium with 10% FCS, 2mM L-glutamine, 1% NEA, antibiotics, 10 nM dexamethasone, 50  $\mu$ g/ml ascorbic acid and 10 mM  $\beta$ -glycero-phosphate [25] and served as "normal cell model".

### Performed tests

#### a) Evaluation of cell proliferation by MTT assay

The proliferation rates were evaluated in GSCs, as well as in non-stem glioblastoma cells and osteoblasts. Cells were cultured at a density of  $5 \times 10^5$  cells in 200  $\mu$ l/well in 96-well microtiter plates and incubated overnight to allow cells to attach to the wells. As shown in Figure 2, cells were divided into 6 arms which were as-

signed to different treatments: no treatment, Met alone, TMZ alone, Soraf alone, Met+TMZ and Met+Soraf. Seventy two hrs after seeding, the MTT test was performed. After removing the medium and washing three times with PBS, the yellow MTT solution [3-(4,5-dimethylthiazolyl-2)-2,5-diphenyltetrazolium bromide] was added and the plate was left at 37 °C for 1 h to allow MTT to be metabolized. Finally, the resulting purple formazan (MTT metabolite product) was resuspended in 200  $\mu$ l DMSO and placed on a shaking table to mix the formazan with the solvent. The reduction of MTT to formazan takes place only when mitochondrial enzymes are active; therefore, the conversion rate can directly estimate the number of living cells. The concentration was determined by optical density at 492 nm by using a fluorescence microplate reader (Synergy 2, BioTek, Winooski, VT, USA). Results derived from the three cell lines were also confirmed through microscopic cell counting.

#### b) Evaluation of oxidative stress parameters in GSCs

##### Reactive oxygen species production by DCF-DA assay

Intracellular ROS production was quantified by

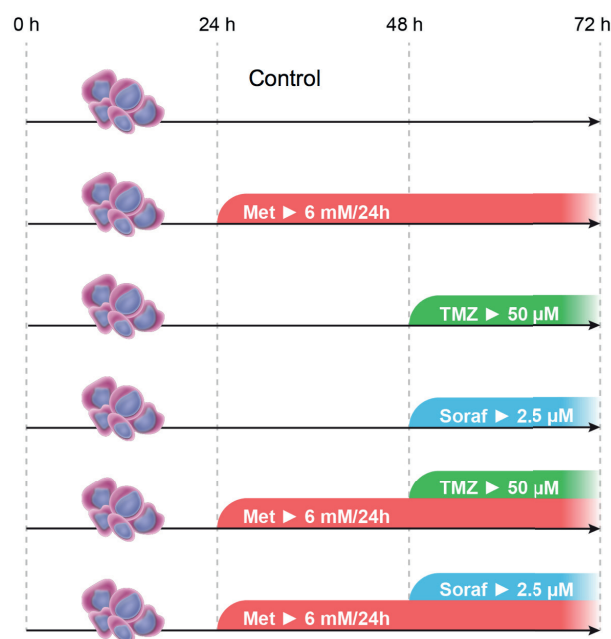


**Figure 2.** Experimental design. Cells were cultured and divided into 6 arms. After 24 hrs, cells received the following treatment: the first arm (control), received no treatment; the 2<sup>nd</sup> arm received 6mM Met/day at 24 and 48 hrs after seeding; the 3<sup>rd</sup> arm received 50  $\mu$ M TMZ at 48 hrs after seeding; the 4<sup>th</sup> arm received 2.5  $\mu$ M Soraf at 48 hrs; the 5<sup>th</sup> arm received 6  $\mu$ M Met/day at 24 and 48 hrs and 50  $\mu$ M TMZ at 48 hrs after seeding; the 6<sup>th</sup> arm received 6  $\mu$ M Met/day at 24 and 48 hrs and 50  $\mu$ M TMZ at 48 hrs. Met: metformin, TMZ: temozolomide, Soraf: sorafenib.

measuring the fluorescence intensity of the cell permeable dye 2',7'-dichlorofluorescein diacetate (DCF-DA) (Molecular Probes Inc, USA), according to the manufacturer instructions. Ninety six well plates were seeded with  $10^6$  cells. Due to the rapid formation of ROS, cells were incubated with the drugs for 1 and 4 hrs before adding the DCF-DA solution. Cell monolayers were washed twice with PBS and stained for 30 min with DCF-DA in the dark, at 37 °C at a final concentration of 2.4 mM. The wells were subsequently washed twice with PBS supplemented with  $Mg^{2+}$  and  $Ca^{2+}$  and fluorescence intensity was measured at 488 nm using a BioTek Synergy 2 fluorescence microplate reader.

#### *Malondialdehyde (MDA) level*

MDA was determined using the fluorometric method with 2-thiobarbituric acid described by Conti et al. [26]. The samples were mixed with a solution of 10 mM 2-thiobarbituric acid in 75 mM  $K_2HPO_4$ , pH 3 solution and heated in a boiling water bath for 1 h. After cooling, the reaction products were extracted in n-butanol. The MDA levels were determined spectrofluorometrically in the organic phase using a synchronous technique with excitation at 534 nm and emission at 548 nm. The MDA values were expressed as nmols/mg protein.

#### *c) Apoptosis assessment by flow cytometry and immunofluorescence microscopy*

Cells were seeded in complete medium at a concentration of  $10^5$  cells/well in a 6-well plate and exposed for 4 and 24 hrs to treatment at the concentrations specified in Table 1. After drug exposure, cells were harvested and washed with cold phosphate-buffered solution and then resuspended in annexin binding buffer. Five  $\mu$ L Alexa Fluor® 488 annexin V and 1  $\mu$ L (100  $\mu$ g/ $\mu$ L) PI working solution (Sigma-Aldrich Chemicals GmbH, St Louis, MO, USA) were added to each 100  $\mu$ L of cell suspension. Cells were then incubated for 15 min in the dark at room temperature, mixed gently with 400  $\mu$ L 1X annexin-binding buffer and then analyzed by flow cytometry, measuring the fluorescence emission at 530 nm (FL1) and  $>575$  nm (FL3) with a BD FACS Canto II flow cytometer. After 24 hrs of drug exposure, cells were also deposited on glass microscope slides and examined using an inverted phase microscope with a 488 nm fluorescence filter for V-annexin Alexa Fluor 488 and for PI. Samples counterstained with an antifade medium containing DAPI (UltraCruz™ Mounting medium-Santa Cruz Biotechnologies) in order to highlight cell nuclei were observed using the 346nm filter (Axiovert, Zeiss, Oberkochen, Germany). Image acquisition was performed using an AxioCam MRC camera.

#### *d) Rhodamine efflux assay*

The fluorescent dye rhodamine 123 is used as a functional assay for cell efflux pump activity [27]. At 24 hrs after treatment,  $5 \times 10^5$  cells were re-suspended

in a solution of rhodamine 123 diluted in PBS (Sigma-Aldrich Chemicals GmbH, St Louis, MO, USA) (1:1000) at a final concentration of 1  $\mu$ g/ml and incubated for 40 min at 37 °C in the dark. Subsequently, the samples were harvested and washed twice by centrifugation for 5 min at 1200 rpm and the resulting pellet was suspended in 300  $\mu$ l PBS with  $Ca^{2+}$  and  $Mg^{2+}$ . After transferring each sample on a 96-well plate, the fluorescence was read at 488 nm by using a BioTek microplate reader.

#### *Statistics*

The data are expressed as the mean $\pm$ standard deviation. All statistical analyses were performed by using the GraphPad Prism software, version 5.0 statistics program (La Jolla, CA, USA). Statistically significant values were obtained by a one-way analysis of variance (ANOVA), with the Bonferroni multiple comparison test (Kruskal-Wallis as nonparametric) and a 95% confidence interval level. Statistical significance was set at  $p < 0.05$ .

## **Results**

#### *a) Metformin combined with sorafenib exerts the highest antiproliferative effects in GSCs and non-stem glioblastoma cells*

As summarized in Figure 3A, in GSCs, significant inhibition of cell proliferation was observed in cells treated with Met alone ( $p < 0.001$ ), Soraf alone ( $p < 0.001$ ) and the combination of Met+Soraf ( $p < 0.001$ ) and Met+TMZ ( $p < 0.001$ ), respectively, as compared to the controls. The most efficient therapy was proven to be the combination between Met and Soraf, which displayed significantly decreased proliferation rates when compared to any other treated arm. Interestingly, TMZ alone failed to offer any benefit and the Met+TMZ combination arm was not statistically different when compared with Met alone ( $p < 0.001$ ) (Figure 3A).

Aside from affecting the number of GSCs and their rate of proliferation, Met also impacted cell shape after 24-48 hrs of drug exposure, as shown in Figure 3B.

In non-stem glioblastoma cells, cell proliferation did not reach any significant statistical difference when treated with either drug alone or even when combined to TMZ ( $p > 0.05$ ). The only efficient therapy seemed to be the combination of Met and Soraf ( $p < 0.001$ ) (Table 1A).

In normal cell lines – osteoblasts, Met alone ( $p > 0.05$ ) did not significantly reduce cell proliferation when compared to the control arm. However, there was a significant reduction of proliferation rate in arms treated with Soraf ( $p < 0.01$ ) and the

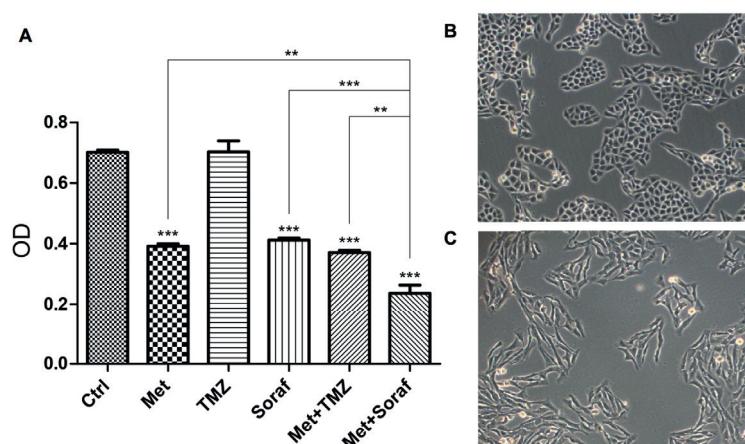


**Figure 3.** GSC proliferation and morphology at 24 and 48 hrs after treatments. **A:** MTT proliferation assay. GSCs were pre-treated with 6  $\mu$ M Met 24 hrs prior to and concomitant with the addition of 2.5  $\mu$ M Soraf or 50  $\mu$ M TMZ. The combination of Met and Soraf was the most efficient therapy in terms of decreased proliferation rates at 24 hrs compared with untreated cells, with either drug alone or with Met+TMZ. Data are statistically significant, as pointed by \*\*  $p < 0.01$  and \*\*\*  $p < 0.001$ . Values are expressed as units of absorbance optical density (OD). **B:** Untreated round-shaped GSCs experienced a morphological change to a fibroblastoid appearance (**C**) after exposure to Met for 48 hrs (white light microscopy,  $\times 10$ )

**Table 1.** MTT proliferation assay performed on non-stem glioblastoma cells and osteoblasts at 24 hrs

	Ctrl	Met	TMZ	Soraf	Met+TMZ	Met+Soraf
A. Non-stem cancer cells						
Mean	0.203	0.189	0.196	0.180	0.214	0.137
SD	0.019	0.017	0.006	0.013	0.007	0.002
p-value			$p > 0.05$			$p < 0.001$
B. Normal cells (osteoblasts)						
Mean	0.159	0.133	0.146	0.103	0.107	0.083
SD	0.025	0.003	0.016	0.003	0.003	0.002
p-value		$p > 0.05$		$p < 0.01$		$p < 0.001$

A. Cell proliferation of non-stem glioblastoma cells at 24 hrs after proposed treatments. Non-stem glioblastoma cells were pre-treated with 6 mM Met 24 hrs prior to and concomitant with the addition of 2.5  $\mu$ M Soraf or 50  $\mu$ M TMZ. MTT cell proliferation assay shows that the combination of Met and Soraf is superior to either treatment alone or compared with Met+TMZ in non-stem glioblastoma cells. Data are statistically significant ( $p < 0.001$ ).

B. Cell proliferation of osteoblasts at 24 hrs after proposed treatments. Osteoblasts were pre-treated with 6 mM Met 24 hrs prior to and concomitant with the addition of 2.5  $\mu$ M Soraf or 50  $\mu$ M TMZ. The combination of drugs and sorafenib monotherapy affected normal osteoblasts. Data are statistically significant, ( $p < 0.01$ ,  $p < 0.001$ ).

combinations Met+TMZ ( $p < 0.01$ ) and Met+Soraf ( $p < 0.001$ ) (Table 1B).

*b) Metformin combined with sorafenib induces ROS production in GSCs*

#### DCF-DA assay

After 1 h of incubation with the drugs, oxidative stress was equally elevated in the arms treated with Met, Met+TMZ and Met+Soraf. There were no differences between the control arm and

the TMZ arm or the Soraf arm. After 4 hrs of incubation with the drugs, Soraf considerably raised the amount of ROS, in the same manner as Met+Soraf. Although the combination between Met+TMZ also maintained increased stress marker values when compared to the control arm, Met+Soraf was more effective in inducing oxidative stress (Figure 4).

#### Malondialdehyde level

Metformin administration increased lipid peroxidation when compared to controls, both

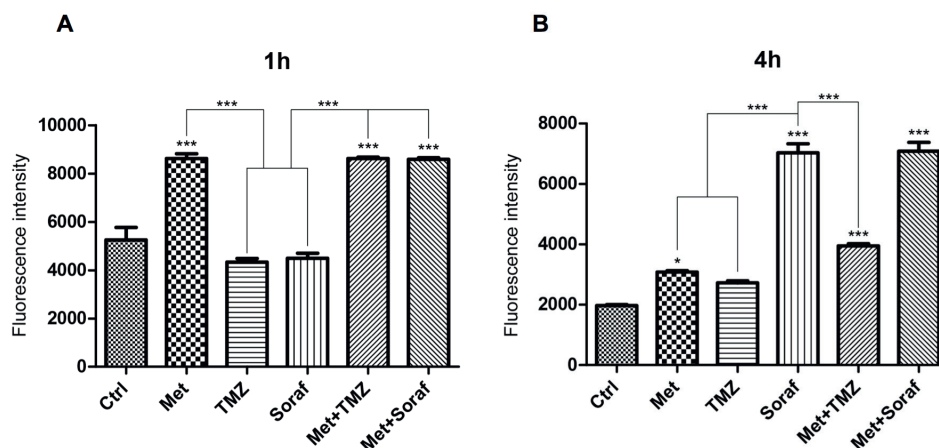


**Figure 4.** DCF-DA performed on GSCs at 1 and 4 hrs of drugs exposure. **A:** The effects of treatments on reactive oxygen species production at 1 hour. ROS formation increased significantly at 1 hour after treatments with Met, Met+TMZ respectively. Met+Soraf compared to control cells or cells treated with TMZ or Soraf (\*\* $p < 0.01$ ; \*\*\*  $p < 0.001$ ). Values are expressed as units of fluorescence. **B:** The effects of treatments on reactive oxygen species production at 4 hrs. ROS formation increased significantly at 4 hrs after treatments with Met and Soraf, respectively. Met+Soraf compared to control cells or cells treated with TMZ (\*  $p < 0.05$ ; \*\*\*  $p < 0.001$ ). Values are expressed as units of fluorescence.

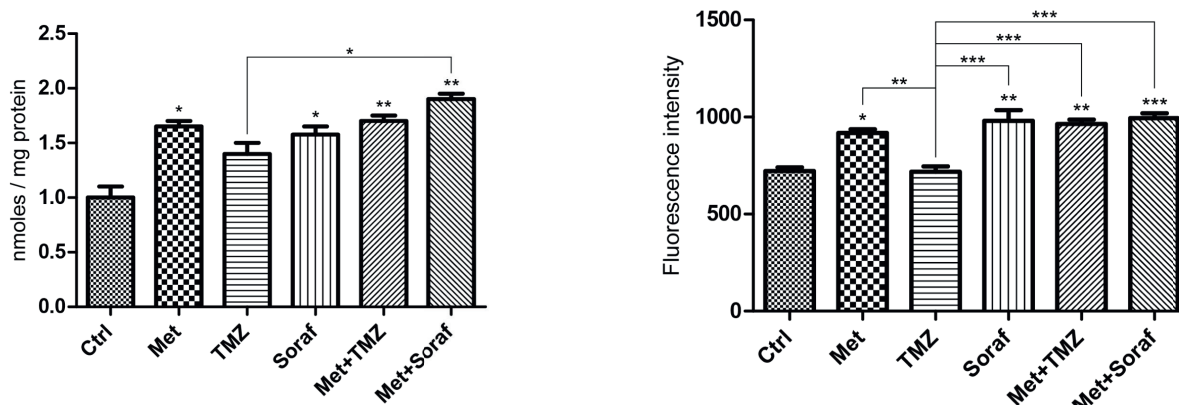


**Figure 5.** Lipid peroxidation assay performed on GSCs at 24 hrs after treatments. MDA levels increased significantly at 24 hrs after treatments with Met and Met+TMZ, respectively. Met+Soraf compared to control cells (\*  $p < 0.05$ ; \*\*  $p < 0.01$ ).

**Figure 7.** Rhodamine 123 assay performed on GSCs 4 hrs after treatments. Rhodamine accumulated significantly within the cells at 4 hrs after treatments with Met, Met+TMZ and Met+Soraf compared to control cells or TMZ treated cells (\*  $p < 0.05$ ; \*\*  $p < 0.01$ ; \*\*\*  $p < 0.001$ ).

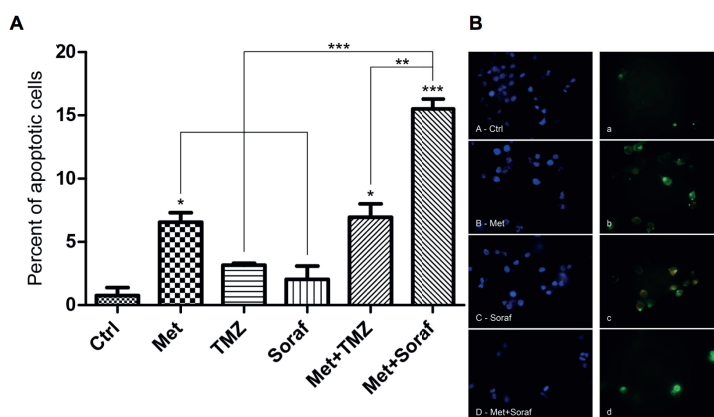


**Figure 6.** Apoptosis induced in GSCs. **A:** Apoptosis assay at 4 hrs performed by flow cytometry. Apoptosis occurred in the arms treated with Met, Met+TMZ and Met+Soraf, with the highest apoptotic rate corresponding to Met+Soraf (\*  $p < 0.05$ ; \*\*  $p < 0.01$ ; \*\*\*  $p < 0.001$ ). **B:** Apoptosis – fluorescence microscopy – 24 hrs after therapy. Cell death was analyzed using annexin-V staining to detect early apoptotic cells, propidium iodide (PI) staining to detect necrotic cells and the staining with both annexin-V and PI to detect late apoptotic cells. *Left panel:* cells were counterstained with DAPI for nuclei (blue) (A-D). *Right panel:* same cells stained with V-Annexin Alexa Fluor488 (green) and PI (red) (a-d). ( $\times 63$  immersion objective Zeiss Axiovert microscope, filter 488 nm).

when used alone ( $p < 0.05$ ) or when combined with TMZ ( $p < 0.01$ ) or with Soraf ( $p < 0.01$ ). The highest values of malondialdehyde corresponded to the lowest proliferation rates obtained with the combination between Met and Soraf (Figure 5).

*c) Metformin combined with sorafenib generates the highest apoptotic rates of GSCs*

The contribution of cell death to the antiproliferative effect of drugs was measured after 4 and 24 hrs of treatment. As shown in Figure 6A, the apoptotic index was shown to be most elevated in the arm treated with Met+Soraf. When compared to the control arm, significant results were obtained in the Met arm and the Met+TMZ ( $p < 0.05$ ) and Met+Soraf arms, respectively ( $p < 0.001$ ). There were no statistically significant differences between the Met and Met+TMZ arms, whereas the combination of Met+Soraf was highly effective in inducing apoptosis when compared to all other arms. Similar results were obtained through fluorescence microscopy, with the observation that Soraf-treated groups had higher levels of late apoptotic cells at 24 hrs (Figure 6B).

*d) Rhodamine 123 efflux assay in treated GSCs*

Low levels of the fluorescent dye rhodamine 123 persisted in the control arm, as well as in the arm treated with TMZ monotherapy, indicating a high efflux capacity. Met monotherapy slightly increased the dye concentration within the cells. Interestingly, the fluorescent dye accumulated in a significantly increased manner when Soraf alone, or when the Met+TMZ or Met+Soraf combinations were used. Thus, the efflux pumps, which are responsible for the expulsion of drugs from cancer cells, seemed to be inhibited when such drug combinations were used (Figure 7).

## Discussion

The failure of existing treatments for glioblastoma has been attributed to the existence of cancer stem-like cells and their high resistance to conventional treatments [28], as well as to their ability to stimulate neoangiogenesis, as previously shown by our research [17]. The existence of drug efflux pumps, which prevent the accumulation of drugs at steady-state levels in tumors, along with the enhanced DNA repair mechanisms in GSCs, contribute to their resistance to therapy [29]. An important determinant of TMZ treatment failure is the increased activity of O-6-methyl-

guanine-DNA methyltransferase (MGMT), a DNA-repair enzyme which removes alkyl groups induced by TMZ from the O6 position of guanine [30]. MGMT is frequently over-expressed in GSCs, most notably in GSCs located in the inner core of the tumor mass [9,31], which could explain their ability to resist chemotherapy.

Our study used stem-like cells, known as TMZ-resistant cells, and attempted to collect initial data on a novel approach that could better target GSCs. As encouraging results have been published linking cancer stem-like cells isolated from glioblastoma and an increased sensitization to Met [17-19] or Soraf [23], we aimed to maximize this antineoplastic effect by associating Met and Soraf in the treatment of glioblastoma cells. The possibility that Met and Soraf could have a synergistic effect is in line with the fact that Met and Soraf target two of the most important signaling cascades frequently dysregulated in glioblastoma, PI3K/AKT/mTOR and RAS/RAF/MAPK axes [32]. These pathways commonly mediate signaling from tyrosine kinase receptors and promote cell proliferation, resistance to cancer therapy and induce an aggressive tumor behavior [33]. The mTOR and MAPK pathways may also be able to relay signals one to another through interactions between member proteins, such as the RAS member of the MAPK pathway, which can induce PI3K activity and thus mTOR signaling. This link may constitute a form of oncologic signaling redundancy, which may explain the reason for the observed failure of tyrosine kinase inhibitors in clinical trials. Clinical trials with EGFR inhibitors or even Soraf in glioblastoma have shown only modest to no advantage in terms of progression free survival [34-36], which supports the hypothesis of Gao et al. that other oncogenic signaling pathways may compensate for the decrease in MAPK signaling [32]. Sorafenib, as a multi-tyrosine kinase inhibitor, may display more potent anti-cancer effects in combination with metformin. First, Soraf decreases tumor angiogenesis through inhibition of VEGFR or PDGFR, a feature of cancer aggressiveness, while also inhibiting RAF, a downstream member of the MAPK signaling pathway. Secondly, Met is an activator of the adenosine monophosphate-activated protein kinase (AMPK), which subsequently inhibits signaling through the PI3K/AKT/mTOR pathway through indirect inhibition of mTOR, while also inhibiting Ras-mediated signaling through PI3K [37].

Since the two molecular pathways affected by Soraf and Met are involved in cell growth and pro-

liferation, we assessed cell viability and proliferation after the proposed treatments. A variability in the response to treatment of different cell lines was observed. Even though our GSC line was resistant to TMZ and was only slightly affected by Soraf monotherapy, it was highly sensitive to the action of Met+Soraf. Interestingly, Met did not affect non-stem glioblastoma cells nor a normal cell line (osteoblasts), indicating a specific action of Met on GSCs. Our observations were also recently confirmed by the *in vitro* study of Wurth et al. [19], which showed that Met selectively reduced the proliferation of the CD133 expressing GSC and impaired tumor-initiating cell spherogenesis. This direct effect on self-renewal mechanisms was associated with a marked inhibition of the Akt-dependent cell survival pathway, while this pathway was not affected in non-stem cells. Also, Met did not have a significant cytotoxic effect on normal umbilical cord-derived mesenchymal stem cells [19].

An interesting result was also the behavior of our GSC cell line under Soraf treatment. While non-stem glioblastoma cells were not significantly impacted by Soraf monotherapy, GSCs exhibited a slight reduction in proliferation, suggesting a certain degree of selectivity of Soraf in targeting GSCs. Our results are in concordance with the study of Carra et al. [23], which highlighted a lower sensitivity of glioblastoma cultures to Soraf after differentiation when compared with the undifferentiated counterpart. Soraf reduced the proliferation of glioblastoma cells and this effect might be partly explained by the inhibition of the PI3K/Akt and MAPK pathways [23].

The cytotoxic effects of Met, Soraf and their association seem to be also related to the production of ROS. After 1 h of incubation with the drugs, Met-treated arms were associated with the highest values of ROS, while at 4 hrs Soraf became the most important generator of ROS. The induction of oxidative stress was further confirmed by the increased levels of lipid peroxidation, a phenomenon known to be associated with oxidative damage [38] and impaired cellular function [39]. At 24 hrs, all treated arms, except for TMZ, showed increased levels of malondialdehyde, confirming a pro-oxidant role of Met and Soraf in GSCs. Our results are consistent with those reported by Isakovic et al. in an *in vivo* murine model and a human glioma-derived cell line where Met administration enhanced the production of ROS and had a synergistic anti-neoplastic effect with hydrogen peroxide, an oxidative stress inducing agent [40].

Although Met possesses anti-oxidant properties in normal cells [41], our results suggest that in cells with sensitive metabolism such as GSCs, Met may in fact act as a pro-oxidant factor, notably when combined with other drugs such as Soraf or TMZ. Increased levels of malondialdehyde were correlated with decreased proliferation rates and increased apoptotic rates.

Apoptosis is a programmed degenerative process triggered by various extracellular or intracellular factors, including oxidative stress. Our results indicate a possible role of oxidative stress in the triggering of apoptotic events, as shown by the increased oxidative stress markers in the Met and Met+Soraf combination arm at 4 hrs after treatments. Soraf however, seems to generate apoptotic events with delay when compared with Met. This is also correlated with a delay in ROS formation when compared to the Met treated arm. In the study of Carra et al., Soraf was confirmed to significantly induce apoptosis/cell death via down regulation of the survival factor Mcl-1 at 24 and 48 hrs after drug exposure [23]. In a chemoradiation scenario, this suggests that the Met-Soraf combination should be given prior rather than after the daily fraction of radiotherapy.

However, the lowered proliferation rates induced by Met and the combination between Met and Soraf are only partly explained by the occurrence of apoptotic death, as the reduced self-renewal capacity of GSCs might also be responsible for the lower proliferation rates. In this respect, Wurth et al. confirmed that Met inhibited GSC self-renewal, as suggested by the decreased levels of spherogenesis, but without reducing overall cell viability [19].

GSCs are known to highly express ATP-binding cassette transporters (ABC transporters), which may partly explain the multi-drug resistant phenotype of these cells [42]. Since both Soraf and Met have been shown to selectively target GSCs, we sought to indirectly assess the activity of such ABC efflux pumps. For this purpose, the fluorescent dye rhodamine-123 was used because of its known role as a substrate for the p-glycoprotein [27]. The results showed that the treatment with Met, Soraf and the combination of Met and TMZ or Soraf led to increased concentrations of rhodamine in cancer cells. Although Met has been shown to be a substrate P-glycoprotein in normal placental cells [43], in MCF-7/adriamycin (MCF-7/adr) cells Met was shown to down-regulate the expression of the P-glycoprotein through the AMPK-mediated inhibition of NF- $\kappa$ B and cAMP

response element (CRE) transcriptional activity [44]. Moreover, Soraf could influence the activity of P-glycoproteins mainly by strongly inhibiting signaling through the RAF/MEK/ERK pathway in multidrug-resistant v-Ha-ras-transformed cells [45]. This suggests a possible synergism between Met and Soraf, which was demonstrated in our study by the increased retention levels of rhodamine 123 within the cells treated with both Met and Soraf.

Also, decreased proliferation rates and decreased activity of ABC transporters, along with the spindle-like morphology change induced by Met (Figure 3B,C) suggested a differentiation process of GSCs. In this regard, Met has been shown to activate FOXO3 via AMPK and consequently to induce differentiation of stem-like glioma-initiating cells *in vitro*, to effectively suppressed their tumor formation capacity *in vivo* and to inhibit the migration of GSC [18,20].

Although our study proposes several hypotheses to explain the observed phenomena, it has several limitations. First, molecular and genetic assays should be performed in order to investigate the expression and activity of signaling pathways and tyrosine kinases involved in the presumed mechanism of action of the drugs involved, as well as molecular phenotyping of the tested cells after drug exposure. Second, since our study employed supraclinical concentrations of metformin, *in vivo* confirmation is required in order to better establish the necessary doses and the possible toxicity of metformin. However, a recent study reported that metformin highly accumulates in

brain parenchyma, even at therapeutic metformin plasma concentration [46]. Also, the combination of Met+Soraf and irradiation warrants further investigation.

## Conclusion

In this study, we reported the first results on the effective combination between Met and Soraf, which notably decreased cell proliferation, increased oxidative stress, inhibited efflux pump activity and finally killed GSCs. Although Met monotherapy and Soraf monotherapy did not affect non-stem glioblastoma cells, the combination between Met and Soraf significantly reduced their proliferation rates. Importantly, Met, although used at higher than therapeutic concentrations, did not affect normal human cells. Thus, Met plus Soraf may become a potent therapy of GSCs, especially for those tumors which are resistant to TMZ. Collectively, our study suggests that GSCs are highly sensitive to the combination of Met and Soraf and that this approach warrants further exploration.

## Acknowledgements

This research was financially supported by a research grant of the Iuliu Hatieganu University of Medicine and Pharmacy (Contract 22714/38/06.10.2011). All the experiments were carried out at the Laboratory of Cell Cultures-Department of Radiobiology and Tumor Biology, Ion Chiricuta Comprehensive Cancer Center in Cluj-Napoca, Romania.

## References

- Wen PY, Kesari S. Malignant gliomas in adults. *NEJM* 2008;359:492-507.
- Niyazi M, Siefert A, Schwarz SB et al. Therapeutic options for recurrent malignant glioma. *Radiother Oncol* 2011;98:1-14.
- Stupp R, Mason WP, van den Bent MJ et al. Radiotherapy plus concomitant and adjuvant temozolomide for glioblastoma. *NEJM* 2005;352:987-996.
- Stupp R, Hegi ME, Mason WP et al. Effects of radiotherapy with concomitant and adjuvant temozolomide versus radiotherapy alone on survival in glioblastoma in a randomised phase III study: 5-year analysis of the EORTC-NCIC trial. *Lancet Oncol* 2009;10:459-466.
- Dimov I, Tasic-Dimov D, Conic I, Stefanovic V. Glioblastoma multiforme stem cells. *Sci World J* 2011;11:930-958.
- Chamberlain MC. Temozolomide: therapeutic limitations in the treatment of adult high-grade gliomas. *Expert Rev Neurother* 2010;10:1537-1544.
- Tomuleasa C, Soritau O, Rus-Ciucu D et al. Functional and molecular characterization of glioblastoma multiforme-derived cancer stem cells. *JBUON* 2010;15:583-591.
- Nakai E, Park K, Yawata T et al. Enhanced MDR1 expression and chemoresistance of cancer stem cells derived from glioblastoma. *Cancer Invest* 2009;27:901-908.
- Pistollato F, Abbadi S, Rampazzo E et al. Intratumoral hypoxic gradient drives stem cells distribution and MGMT expression in glioblastoma. *Stem Cells* 2010;28:851-862.
- Schlegel J, Merdes A, Stumm G et al. Amplification of the epidermal-growth-factor-receptor gene correlates with different growth behaviour in human glioblastoma. *Int J Cancer* 1994;56:72-77.
- Narita Y, Nagane M, Mishima K, Huang HJ, Furnari FB, Cavenee WK. Mutant epidermal growth factor receptor signaling down-regulates p27 through activation of the

- phosphatidylinositol 3-kinase/Akt pathway in glioblastomas. *Cancer Res* 2002; 62:6764-6769.
12. Xu C, Wu X, Zhu J. VEGF promotes proliferation of human glioblastoma multiforme stem-like cells through VEGF receptor 2. *Sci World J* 2013;2013:413-417.
  13. Kim Y, Kim E, Wu Q et al. Platelet-derived growth factor receptors differentially inform intertumoral and intratumoral heterogeneity. *Genes Develop* 2012;26:1247-1262.
  14. Soroceanu L, Kharbanda S, Chen R et al. Identification of IGF2 signaling through phosphoinositide-3-kinase regulatory subunit 3 as a growth-promoting axis in glioblastoma. *Proc Natl Acad Sciences USA* 2007;104:3466-3471.
  15. Puputti M, Tynninen O, Sihto H et al. Amplification of KIT, PDGFRA, VEGFR2, and EGFR in gliomas. *Mol Cancer Res* 2006;4:927-934.
  16. Robinson JP, Vanbrocklin MW, McKinney AJ, Gach HM, Holmen SL. Akt signaling is required for glioblastoma maintenance in vivo. *Am J Cancer Res* 2011;1:155-167.
  17. Soritau O, Tomuleasa C, Aldea M et al. Metformin plus temozolomide-based chemotherapy as adjuvant treatment for WHO grade III and IV malignant gliomas. *JBUON* 2011; 16:282-289.
  18. Sato A, Sunayama J, Okada M, et al. Glioma-initiating cell elimination by metformin activation of FOXO3 via AMPK. *Stem Cells Transl Med* 2012;1:811-824.
  19. Wurth R, Pattarozzi A, Gatti M et al. Metformin selectively affects human glioblastoma tumor-initiating cell viability: A role for metformin-induced inhibition of Akt. *Cell Cycle* 2013;12:145-156.
  20. Ferla R, Haspinger E, Surmacz E. Metformin inhibits leptin-induced growth and migration of glioblastoma cells. *Oncology Lett* 2012;4:1077-1081.
  21. Dowling RJ, Zakikhani M, Fantus IG, Pollak M, Sonenberg N. Metformin inhibits mammalian target of rapamycin-dependent translation initiation in breast cancer cells. *Cancer Res* 2007;67:10804-10812.
  22. Gomez-Pinillos A, Ferrari AC. mTOR signaling pathway and mTOR inhibitors in cancer therapy. *Hematol Oncol Clin North Am* 2012;26:483-505.
  23. Carra E, Barbieri F, Marubbi D et al. Sorafenib selectively depletes human glioblastoma tumor-initiating cells from primary cultures. *Cell Cycle* 2013;12:491-500.
  24. Wilhelm SM, Carter C, Tang L et al. BAY 43-9006 exhibits broad spectrum oral antitumor activity and targets the RAF/MEK/ERK pathway and receptor tyrosine kinases involved in tumor progression and angiogenesis. *Cancer Res* 2004;64:7099-7109.
  25. Tomuleasa CI, Foris V, Soritau O et al. Effects of 60Co gamma-rays on human osteoprogenitor cells. *Roman J Morphol Embryol* 2009;50:349-355.
  26. Conti M, Morand PC, Levillain P, Lemonnier A. Improved fluorometric determination of malonaldehyde. *Clin Chem* 1991;37:1273-1275.
  27. Lee JS, Paull K, Alvarez M et al. Rhodamine efflux patterns predict P-glycoprotein substrates in the National Cancer Institute drug screen. *Mol Pharmacol* 1994;46:627-638.
  28. Orza A, Soritau O, Tomuleasa C et al. Reversing chemoresistance of malignant glioma stem cells using gold nanoparticles. *Int J Nanomed* 2013;8:689-702.
  29. Liu G, Yuan X, Zeng Z et al. Analysis of gene expression and chemoresistance of CD133+ cancer stem cells in glioblastoma. *Mol Cancer* 2006; 5:67.
  30. Fouse SD, Nakamura JL, James CD, Chang S, Costello JF. Response of primary glioblastoma cells to therapy is patient specific and independent of cancer stem cell phenotype. *Neurooncology* 2014; 16: 361-371.
  31. Ropolo M, Daga A, Griffero F et al. Comparative analysis of DNA repair in stem and nonstem glioma cell cultures. *Mol Cancer Res* 2009;7:383-392.
  32. Gao Q, Lei T, Ye F. Therapeutic targeting of EGFR-activated metabolic pathways in glioblastoma. *Expert Opin Investig Drugs* 2013;22:1023-1040.
  33. Cheng CK, Fan QW, Weiss WA. PI3K signaling in glioma-animal models and therapeutic challenges. *Brain Pathol* 2009;19:112-120.
  34. Peereboom DM, Ahluwalia MS, Ye X et al. NABTT 0502: a phase II and pharmacokinetic study of erlotinib and sorafenib for patients with progressive or recurrent glioblastoma multiforme. *Neurooncology* 2013;15:490-496.
  35. Hainsworth JD, Ervin T, Friedman E et al. Concurrent radiotherapy and temozolomide followed by temozolomide and sorafenib in the first-line treatment of patients with glioblastoma multiforme. *Cancer* 2010;116:3663-3669.
  36. Hegi ME, Diserens AC, Bady P et al. Pathway analysis of glioblastoma tissue after preoperative treatment with the EGFR tyrosine kinase inhibitor gefitinib—a phase II trial. *Mol Cancer Ther* 2011;10:1102-1112.
  37. Polivka J, Jr, Janku F. Molecular targets for cancer therapy in the PI3K/AKT/mTOR pathway. *Pharmacol Ther* 2013; pii: S0163-7258 (13): 00240-4.
  38. Haugaard N. Cellular mechanisms of oxygen toxicity. *Physiol Rev* 1968;48:311-375.
  39. Halliwell B. Lipid peroxidation, antioxidants and cardiovascular disease: how should we move forward? *Cardiovasc Res* 2000;44:10-418.
  40. Isakovic A, Harhaji L, Stevanovic D et al. Dual anti-glioma action of metformin: cell cycle arrest and mitochondria-dependent apoptosis. *Cell Mol Life Sci* 2007;64:1290-1302.
  41. Mirmiranpour H, Mousavizadeh M, Noshad S et al. Comparative effects of pioglitazone and metformin on oxidative stress markers in newly diagnosed type 2 diabetes patients: a randomized clinical trial. *J Diabetes Complic* 2013;27:501-507.
  42. Riganti C, Salaroglio IC, Caldera V et al. Temozolomide downregulates P-glycoprotein expression in glioblastoma stem cells by interfering with the Wnt3a/glycogen synthase-3 kinase/beta-catenin pathway. *Neurooncology* 2013;15:1502-1517.
  43. Hemauer SJ, Patrikeeva SL, Nanovskaya TN, Hankins GD, Ahmed MS. Role of human placental apical membrane transporters in the efflux of glyburide, rosiglitazone, and metformin. *Am J Obstet Gynecol* 2010;202:385 e1-7.
  44. Kim HG, Hien TT, Han EH et al. Metformin inhibits P-glycoprotein expression via the NF-kappaB pathway and CRE transcriptional activity through AMPK activation. *Br J Pharmacol* 2011;162:1096-1108.
  45. Eum KH, Ahn SK, Kang H, Lee M. Differential inhibitory effects of two Raf-targeting drugs, sorafenib and PLX4720, on the growth of multidrug-resistant cells. *Mol Cell Biochem* 2013;372:65-74.
  46. Labuzek K, Suchy D, Gabryel B, Bielecka A, Liber S, Okopien B. Quantification of metformin by the HPLC method in brain regions, cerebrospinal fluid and plasma of rats treated with lipopolysaccharide. *Pharm Rep* 2010; 62: 956-965.